miR-382-3p downregulation contributes to the carcinogenesis of lung adenocarcinoma by promoting AKT SUMOylation and phosphorylation

HUA FANG[1*], WEIHUA WU[2*] and ZHIJUN WU[3]

[1]Department of Oncology, Fuxing Hospital, Capital Medical University, Beijing 100038; [2]Department of Oncology, Beijing Chest Hospital, Capital Medical University, Beijing 101149; [3]Department of Oncology, Ongniud Banner Hospital, Chifeng, Inner Mongolia Autonomous Region 024500, P.R. China

Received September 30, 2021; Accepted February 8, 2022

DOI: 10.3892/etm.2022.11367

Abstract. Lung adenocarcinoma (LA), the primary histological type of non-small cell lung cancer, is still incurable; its diagnosis and treatment remain a major clinical challenge. A previous study by our group examined the microRNA (miRNA/miR) expression profile in the extracellular vesicles from patients with LA and healthy controls and indicated that miR-382-3p levels were reduced in patients with LA. However, the precise roles of miR-382-3p in LA have so far remained elusive. In the present study, the miR-382-3p levels in tumor and adjacent non-tumor control samples from 78 patients with LA were examined and it was identified that miR-382-3p expression was reduced in LA tumor samples compared with that in adjacent non-tumor control tissues (P=0.022). Furthermore, miR-382-3p overexpression inhibited LA growth in a xenograft mouse model. Prediction results indicated that miR-382-3p may regulate protein ubiquitination and SUMOylation. Small ubiquitin-like modifier (SUMO)1 activating enzyme subunit 1 (SAE1), one of the key components of the SUMO-activating complex, was identified as a direct target of miR-382-3p via dual-luciferase and immunoblotting assays. In patients with LA, miR-382-3p expression was negatively correlated with SAE1 protein levels (r=-0.39, P<0.05) and higher SAE1 expression contributed to poor prognosis (P<0.01). Using immunoprecipitation, it was identified that miR-382-3p reduction-induced SAE1 overexpression upregulated AKT SUMOylation, which further promoted AKT phosphorylation and activated the AKT signaling pathway. miR-382-3p inhibition promoted proliferation and inhibited apoptosis in LA cell lines, which was restored by SAE1 knockdown. In conclusion, the present study revealed that downregulation of miR-382-3p contributed to the carcinogenesis of LA via upregulation of SAE1 and promotion of AKT SUMOylation, providing a candidate target for LA treatment.

Correspondence to: Dr Hua Fang, Department of Oncology, Fuxing Hospital, Capital Medical University, 20 Fu Xing Men Wai Street, Beijing 100038, P.R. China
E-mail: laifu750130@126.com

*Contributed equally

Key words: lung adenocarcinoma, microRNA, SUMOylation, SAE1

Introduction

Lung cancer ranks first in incidence among malignancies and remains the most common cause of cancer-associated mortality in China. Lung adenocarcinoma (LA) is the most common type of primary lung cancer, accounting for >40% of all lung cancer cases (1). Although efforts have been made to understand the molecular characteristics of LA and develop novel screening and treatment strategies for the disease, most patients are diagnosed at an advanced stage due to a lack of effective diagnostic approaches (2,3). Hence, searching for novel biomarkers to diagnose and treat LA is an urgent concern.

MicroRNAs (miRNAs/miRs) are a group of small non-coding RNAs that negatively regulate gene expression by directly targeting the 3'-untranslated region (UTR) of mRNA. miRNAs have important roles in maintaining normal physiological conditions in the human body. Abnormal miRNA expression has been indicated to be related to multiple human diseases, including lung cancer (4-6). A previous study by our group identified that miR-382-3p was downregulated in the extracellular vesicles from the peripheral blood of 153 patients with LA (7). However, the mechanisms of how miR-382-3p downregulation is related to LA have remained elusive.

Activation of PI3K/Akt signaling has been confirmed as a major signaling event in carcinogenesis (8). Tsurutani *et al* (9) examined phosphorylated (p)AKT levels in 300 non-small cell lung cancer (NSCLC) specimens and 100 adjacent lung tissue specimens and determined that AKT activation was specific for NSCLC tumors vs. the adjacent tissue (73.4 vs. 0%; P<0.05). They also observed that AKT activation was more frequent in adenocarcinomas than in squamous cell carcinomas of the lung (78.1 vs. 68.5%; P=0.04) and was associated with shorter overall survival for all stages of the disease (log-rank P=0.04). Yoshizawa *et al* (10) reported that pAKT is overexpressed

in 78% of NSCLCs. Once again, pAKT was detected more frequently in adenocarcinomas (43%) than in squamous cell carcinomas (36%), but this observation was not statistically significant. The 5-year survival rate was significantly lower in patients with pAKT-positive tumors. Lysine modification has been reported to be critical for the phosphorylation, subcellular localization, stability and activity of Akt. Furthermore, Akt has been indicated to be modified via SUMOylation at multiple sites, which is required for its kinase activity and biological function (11).

SUMOylation is a modification process that involves the addition of small ubiquitin-like modifier (SUMO) to the acceptor lysine of target proteins. This modification process consists of three enzymatic cascade steps: An activation step [heterodimer E1 enzymes SUMO1 activating enzyme subunit 1 (SAE1) and SAE2], a conjugation step (E2 enzyme Ubc9) and a substrate modification step (cooperation of the E2 and E3 enzymes) (12). Dysregulated SUMOylation processes are usually found in cancers as one of the most important physiological mechanisms in cellular response to stress (13).

It has been reported that SAE1 overexpression is related to poor prognosis of patients with multiple types of cancer, suggesting that SUMOylation may be involved in the progression of malignant tumors. In addition, the mRNA level of SAE1 was positively correlated with lymph node metastasis in patients with LA (14). However, the mechanism by which SAE1 contributes to the progression of LA remains elusive. The present study aimed to investigate the relationship between miR-382-3p dysregulation and LA carcinogenesis. The expression of miR-382-3p in tumor and non-tumor control tissue samples from 78 patients with LA was examined and the biological function and the underlying mechanisms of miR-382-3p during the carcinogenesis of LA were identified.

Materials and methods

Patients. A cohort consisting of 78 patients with LA (age, 54-71 years; females/males, 33/45) and 59 healthy controls (age, 45-74 years; females/males, 26/33) was included in this study. All participants were recruited at Fuxing Hospital, Capital Medical University (Beijing, China) between February 2017 and July 2018. Inclusion criteria: The LA cases were diagnosed as stage I/II according to the eighth edition of the Union for International Cancer Control Tumor-Node-Metastasis system and confirmed via histopathological analysis (6). Exclusion criteria: Patients with history of thoracic surgery; with other tumors; complicated with severe liver dysfunction and kidney dysfunction; with acute pulmonary infection, connective tissue diseases, infectious diseases, metabolic diseases, hematopoietic dysfunction and patients with mental illness or a family history of mental illness, pregnant or lactating women.

The present study was approved by the Human Basic and Clinical Research Ethics Committee of Fuxing Hospital (Beijing, China; approval no. 2018FXHEC-KY-19). Written informed consent was obtained from all the participants. The privacy of the subjects was protected, according to the Declaration of Helsinki.

Xenograft mouse model. A total of 24 female NOD-SCID mice (age, 5 weeks; body weight, 15-20 g) were purchased from the Charles River Laboratories, Inc. All mice were housed at 23-25˚C with 50-60% humidity, a 12-h light/dark cycle and food and water *ad libitum*. To establish the xenograft mouse model, a total of $5x10^6$ A549-miR-382-3p or H1299-miR-382-3p cells in 100 μl PBS together with an equal volume of Matrigel® basement membrane matrix were subcutaneously injected into the right flanks of the mice (3 mice in each group). Tumors were measured every 7 days with a caliper and the tumor volume (mm^3) was calculated as 0.5 x length x $width^2$. Regarding the tumor burden, a marked increase in tumor size (≥10% body weight) was applied as a humane endpoint. Mice were euthanized using CO_2 with the flow rate for CO_2 set at 30% chamber volume displaced per minute. Death of the mice was verified by observation of respiratory arrest, cessation of heartbeat (lack of activity for ≥5 min) and pupillary response to light. All animal protocols were performed strictly according to the relevant National Institutes of Health Guidelines for the Care and Use of Laboratory Animals (15,16). All experiments involving animals were pre-approved by the Institutional Animal Care and Use Committee (IACUC) of Fuxing Hospital (Beijing, China).

Cell culture. The normal human lung fibroblast cell lines MRC-9 (CCL-212) and WI-38 (CCL-75) cells were purchased from the American Type Culture Collection and cultured in Eagle's minimum essential medium (Hyclone; Cytiva) containing 10% fetal bovine serum (Hyclone; Cytiva), 100 IU/ml penicillin and 100 IU/ml streptomycin. Human embryonic kidney 293T cells (1101HUM-PUMC000091) and the human non-small cell lung carcinoma cells lines A549 (1101HUM-PUMC000002), H1299 (1101HUM-PUMC000469), Calu-3 (1101HUM-PUMC000032), NCI-H1975 (1101HUM-PUMC000252), NCI-H2087 (1101HUM-PUMC000253) and SK-LU-1 (1101HUM-PUMC000237) were obtained from China Infrastructure of Cell Line Resources and cultured in Dulbecco's Modified Eagle's medium (Hyclone; Cytiva) containing 10% fetal bovine serum (Hyclone; Cytiva), 100 IU/ml penicillin and 100 IU/ml streptomycin. All cells were maintained at 37˚C in a humidified atmosphere containing 5% CO_2. For functional studies, A549 (p53 wild-type) and H1299 (p53 deleted) cells were selected due to their miR-382-3p levels and p53 expression.

RNA extraction. Total RNA was extracted from tissues or cell samples using TRIzol reagent (Invitrogen; Thermo Fisher Scientific, Inc.) following the manufacturer's protocol. In brief, samples were homogenized in 1 ml TRIzol mixed with 200 μl chloroform. After centrifugation, the supernatants were transferred into a new tube and the RNA was precipitated with isopropanol. The RNA pellets were dissolved using RNase-free water after washing with 70% ethanol and the RNA concentration and purity were determined using a NanoDrop-2000 spectrophotometer (Thermo Fisher Scientific, Inc.). RNA purity was determined through the absorbance ratio at 260 nm/280 nm and 260 nm/230 nm. Only high-purity RNA samples (260 nm/280 nm ~2.0 and 260 nm/230 nm between 1.9 and 2.2) were included in this study.

Reverse transcription-quantitative PCR (RT-qPCR). Cyclin D1 (CCND1), cyclin-dependent kinase (CDK2) and p21 mRNA levels were determined via RT-qPCR. In brief,

cDNA was synthesized using a RevertAid first-strand cDNA synthesis kit (Thermo Fisher Scientific, Inc.) following the manufacturer's protocol. The expression of candidate genes was quantified via qPCR using SYBR-Green PCR master mix (Thermo Fisher Scientific, Inc.) using 95˚C for 10 min as the initial denaturation, and with 40 cycles at 95˚C for 15 sec and 60˚C for 1 min. GAPDH was used as a loading control.

For miRNA quantification, single-strand cDNA was synthesized using a TaqMan MicroRNA Reverse Transcription Kit (Applied Biosystems; Thermo Fisher Scientific, Inc.) with miRNA-specific primers. The levels of candidate miRNAs were determined by using TaqMan Universal PCR Master Mix (Applied Biosystems; Thermo Fisher Scientific, Inc.) and miRNA-specific TaqMan MGB probes (Applied Biosystems; Thermo Fisher Scientific, Inc.). The small nuclear RNA U6 was used as a loading control.

Each sample in each group was measured in triplicate and the experiment was repeated at least three times. Relative gene levels were compared using the $2^{-\Delta\Delta Cq}$ method (17).

Primer sequences were as follows: CDK2 forward, 5'-GCC TAGCTTTCTGCCATTCT-3' and reverse, 5'-GTCCAAAGT CTGCTAGCTTGAT-3'; CCND1 forward, 5'-CCTCGGTGT CCTACTTCAAATG-3' and reverse, 5'-CACTTCTGTTCC TCGCAGAC-3'; p21 forward, 5'-GCGACTGTGATGCGC TAAT-3' and reverse, 5'-GTGGTGTCTCGGTGACAAAG-3'; GAPDH forward, 5'-GGTGTGAACCATGAGAAGTAT GA-3' and reverse, 5'-GAGTCCTTCCACGATACCAAAG-3', miR-382-3p forward, 5'-CTAATCATTCACGGACAA-3' and reverse, 5'-GTGCAGGGTCCGAGGT-3'; U6 forward, 5'-TGG AACGCTTCACGAATTTGCG-3' and reverse, 5'-GGA-ACG ATACAGAGAAGATTAGC-3'.

Dual-luciferase assay. The full length of the 3'-UTR of SAE1 was amplified by PCR using 293T cell genomic DNA as template. The primers sequences were: SAE1-Nhe forward, 5'-CTAGCTAGCACTCAAGATTTGGCAGCC CCAGAGA-3' and SAE1-Xho reverse, 5'-CCGCTCGAGTCA GAATAGGAAAGAGACTGATTTATTGA-3'. The amplification cycle using 95˚C 10 min as the initial denaturation with 25 cycles at 95˚C for 10 min, 95˚C for 15 sec and 60˚C for 1 min. The product was cloned downstream of the Firefly luciferase gene into a pmirGLO plasmid (Promega Corporation), between Nhe I and Xho I sites, to generate the reporter vector. The mutant vector generation was processed using Fast MultiSite Mutagenesis System kit (TransGen Biotech Co., Ltd.) and mutant primers (SAE1-Mu forward, 5'-GTTCTTTTTAAA AGAAATATAATAAAGTTACTTG-3', and 5'-SAE1-Mu reverse, TTATTATATTTCTTTTAAAAAGAACCAAGGA AAA-3'. miR-382-3p mimics, inhibitor and sequence-scrambled single- and double-strand control oligos were purchased from Shanghai GenePharma Co., Ltd. 293T cells were seeded into 48-well plates at $5x10^4$ cells/well and allowed to attach overnight for the luciferase reporter assays. The reporter vector was co-transfected into the cells with miRNA mimics or inhibitor using Lipofectamine® 2000 (Invitrogen; Thermo Fisher Scientific, Inc.) following the manufacturer's protocol. In brief, the nucleotides were mixed with medium-diluted Lipofectamine and then incubated at 25˚C for 20 min. The nucleotide-Lipofectamine complexes were added to each well containing cells and medium and gently mixed by rocking the plate back and forth. The cells were incubated at 37˚C in a CO_2 incubator for 6 h and then the complexes were removed. At 48 h after transfection, the cells were lysed and the luciferase activity was analyzed using a Dual-Luciferase® Reporter Assay System (Promega Corporation). Experiments were performed in triplicate and the results were expressed as the relative luciferase activity (Firefly luciferase/*Renilla* luciferase).

The sequences were as follows: miR-382-3p mimics, 5'-AAUCAUUCACGGACAACACUU-3'; mimics control, 5'-AGUGUUGGACUAAGCGGAGGUA-3'; miR-382-3p inhibitor, 5'-AAGUGUUGUCCGUGAAUGAUU-3'; inhibitor control, 5'-UAACACGUCUAUACGCCCA-3'.

Immunoprecipitation (IP). Cells were harvested and lysed with IP buffer containing 20 mM Tris (pH 7.5), 150 nM NaCl, 1% Triton X-100, a protease inhibitor cocktail and 20 mM N-ethylmaleimide. Next, 2 mg of the cellular supernatant was incubated overnight with a complex of anti-SUMO1 antibody (cat. no. ab32058; Abcam) and protein-A beads to enrich SUMOylated proteins at 4˚C. After washing four times with Tris-buffered saline (TBS), the protein complexes were eluted with sample loading buffer for immunoblotting.

Protein extraction. Tumor and non-tumor control samples from 72 patients with LA were used for protein extraction (for six patients, samples were insufficient for protein extraction). To extract proteins from tissue samples, the frozen tissue was mixed and homogenized in ice-cold RIPA lysis and extraction buffer (Thermo Fisher Scientific, Inc.) containing protease inhibitors (Thermo Fisher Scientific, Inc.) and then centrifuged at 16,000 x g for 20 min at 4˚C.

To extract proteins from cells, the spent medium in the culture dishes was discarded, and the cells were washed with ice-cold PBS. The cells were then lysed by adding ice-cold RIPA lysis and extraction buffer (Thermo Fisher Scientific, Inc.) containing protease inhibitors (Thermo Fisher Scientific, Inc.). The cells were collected using a cold plastic cell scraper and then subjected to centrifugation at 16,000 x g for 20 min at 4˚C. The total protein concentration was determined using a Pierce™ BCA Protein Assay Kit (Thermo Fisher Scientific, Inc.) and the protein was stored at -80˚C until use.

Immunoblotting. From each sample, 20 μg of protein were loaded and separated using 10% SDS-PAGE and then blotted onto a polyvinylidene fluoride membrane (EMD Millipore) via electrophoretic transfer. The membranes were blocked with 5% nonfat milk (BD Biosciences) and incubated with one of the primary antibodies overnight at 4˚C. After incubation with the corresponding horseradish peroxidase (HRP)-conjugated secondary antibodies (1:5,000 dilution) for another 2 h at room temperature, the signals were detected using an enhanced chemiluminescence kit (Thermo Fisher Scientific, Inc.). The GAPDH signal was used for normalization. The following antibodies were used: Rabbit anti-SAE1 polyclonal antibody (cat no. 13585S; 1:1,000 dilution; Cell Signaling Technology, Inc.), rabbit anti-SUMO1 polyclonal antibody (cat no. 4930S; 1:2,000 dilution; Cell Signaling Technology, Inc.), rabbit anti-pAkt (Ser473) polyclonal antibody (cat no. 4060S; 1:2,000 dilution; Cell Signaling Technology, Inc.), mouse anti-GAPDH monoclonal antibody (cat no. sc-47724; 1:2,000

dilution; Santa Cruz Biotechnology, Inc.). HRP conjugated goat anti-rabbit antibody (1:5,000; cat no. 7074; Cell Signaling Technology, Inc.), HRP conjugated goat anti-mouse antibody (1:5,000; cat no. 7076; Cell Signaling Technology, Inc.).

Small interfering (si)RNA transfection. siRNA targeting SAE1 or control RNA (RiboBio Co., Ltd.) was transfected into cells by using Lipofectamine 2000 (Thermo Fisher Scientific, Inc.) following the manufacturer's protocol. In brief, the nucleotides were mixed with medium-diluted Lipofectamine® and then incubated at 25˚C for 20 min. The nucleotide-Lipofectamine® complexes were added to each well containing cells and medium, with a final concentration of 20 nM, and gently mixed by rocking the plate back and forth. The cells were incubated at 37˚C in a CO_2 incubator for 6 h and then the complexes were removed. At 48 h after transfection, the cells were subjected to a cell proliferation assay. The sequence were as follows: siSAE1, 5'-AGACAACGATGGTCAAAAA-3'; and siRNA control, 5'-GAGACTAAGAACGAACTAA-3'.

Cell proliferation assay. An MTT assay was employed to determine cell viability. In brief, $2x10^3$ A549 or H1299 cells were seeded into each well of a 96-well plate and allowed to attach overnight. siRNA targeting SAE1 or the control RNA was transfected into the cells separately for 48 h and subsequently, 20 μl of MTT (5 mg/ml; MilliporeSigma) was added to each well. After incubation for 4 h, the medium was discarded followed by the addition of DMSO to each well. The absorbance at 570 nm was recorded using Multiskan™ FC Microplate Photometer (Thermo Fisher Scientific, Inc.).

Cell apoptosis assay. Apoptotic cells were analyzed by flow cytometry after staining with FITC-Annexin V and propidium iodide (cat no. 640914; BioLegend, Inc.). Briefly, cells were washed twice with cold Cell Staining buffer, and then resuspended in Annexin V Binding buffer at a concentration of $5x10^6$ cells/ml. Add 5 μl of FITC-Annexin V and 10 μl of propidium iodide solution into 100 μl of cell suspension, and then the cells were gently vortexed and incubated for 15 min at 25˚C in the dark. Add 400 μl of Annexin V Binding Buffer to each tube and then the cells were subjected to flow cytometry analysis using FACSCanto Plus instrument (BD Biosciences). The results were analyzed using FlowJo software (v.10.4.1; Tree Star, Inc.).

Immunohistochemistry. Paraffin-embedded sections were first deparaffinized and then heated in a microwave oven with 10% citrate buffer for 10 min twice and cooled to room temperature. After blocking with 5% BSA was for 30 min at 25˚C, the slides were incubated with rabbit anti-Ki-67 polyclonal antibody (cat. no. ab16667; 1:500 dilution; Abcam) or rabbit anti-SAE1 polyclonal antibody (cat. no. ab38434; 1:500 dilution; Abcam) at 4˚C overnight. After three washes with TBS containing Tween-20 (TBST), the sections were incubated with HRP-conjugated goat anti-rabbit secondary antibody (cat. no. ab6721; 1:2,500 dilution; Abcam). The sections were washed with TBST three times and the signals were detected using a DAB Substrate kit following the manufacturer's protocol. Images were obtained using a microscope (DM2000; Leica Microsystems GmbH).

Table I. Characteristics of the patients with lung adenocarcinoma included in this study (n=78).

Variable	Value
Sex	
Male	45 (57.7)
Female	33 (42.3)
Age, years	63.00±8.52
Smoking	
No	22 (28.2)
Yes	56 (71.8)
Clinical stage	
IA	16 (20.5)
IB	22 (28.2)
IIA	18 (23.1)
IIB	22 (28.2)

Values are expressed as n (%) or the mean ± standard deviation.

The intensity of staining (0, negative; 1, weak; 2, moderate; 3, strong) and percentage of tumor cells showing staining (0-100%) were evaluated independently. An H-score of 0-300 was generated by multiplying the intensity of positivity by the percentage of tumor cells with staining.

Statistical analysis. Data were analyzed using the SPSS statistical package (version 19.0; IBM Corporation). A paired t-test was used to compare the relative miR-382-3p levels between tumors and non-tumor tissues, miR-382-3p levels in established miR-382-3p overexpressing cell lines and control cells, as well as miR-382-3p and mRNA levels in miR-382-3p inhibitor or inhibitor control-transfected cells. One-way ANOVA was used as a multiple-comparisons test to analyze datasets containing more than two groups with a subsequent Tukey's post-hoc test for comparison between two groups. Pearson's correlation analysis was used to determine the correlation coefficient between miR-382 levels and SAE1 protein levels. The survival of different groups of patients was analyzed using the Kaplan-Meier method with the log-rank test. $P<0.05$ was considered to indicate statistical significance.

Results

miR-382-3p is downregulated in patients with LA and functions as a tumor suppressor in LA. To investigate whether miR-382-3p is related to the carcinogenesis of LA, miR-382-3p levels in tumor samples and adjacent non-tumor tissues from 78 patients with LA (age, 63.00±8.52 years old; male:female, 45/33; Table I) were analyzed. miR-382-3p levels in normal lung fibroblasts and six LA cell lines were also examined. As presented in Fig. 1A and B, the levels of miR-382-3p were significantly decreased in LA tumors and cell lines, suggesting that miR-382-3p downregulation may contribute to the carcinogenesis of LA.

To understand the function of miR-382-3p in LA cells, A549 cells that had the lowest expression of miR-382-3p and

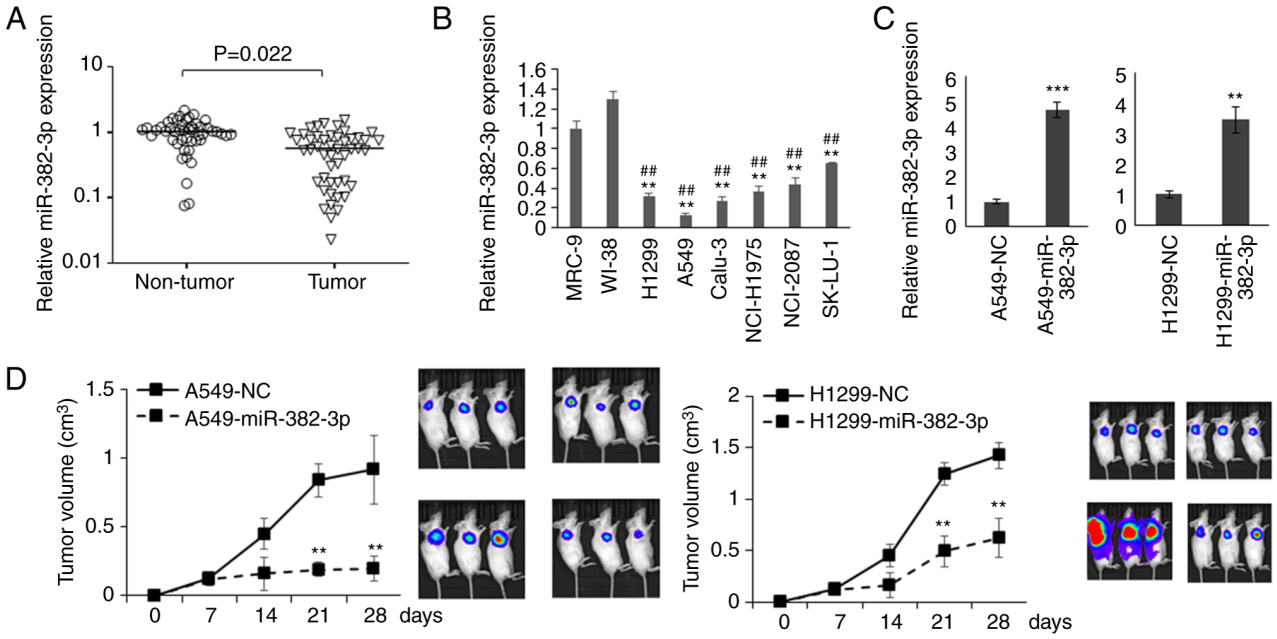

Figure 1. miR-382-3p is downregulated in LA samples and LA cell lines. (A) miR-382-3p levels in LA samples and adjacent non-tumor tissues were determined by RT-qPCR. (B) miR-382-3p levels in normal lung fibroblasts and LA cell lines were measured by RT-qPCR. **P<0.01 vs. MRC-9; $^{\#\#}$P<0.01 vs. WI-38. (C) miR-382-3p levels in miR-382-3p overexpression A549 and H1299 cell lines were examined by RT-qPCR. (D) miR-382-3p-overexpressing A549 and H1299 cells were subcutaneously injected into NOD-SCID mice. Tumor growth was monitored every week. **P<0.01, ***P<0.001 vs. NC. NC, negative control; RT-qPCR, reverse transcription-quantitative PCR; miR, microRNA; LA, lung adenocarcinoma.

H1299 cells lacking the expression of p53 protein were used to construct miR-382-3p-overexpressing cell lines to generate a xenograft mouse model (Fig. 1C). As presented in Fig. 1D and, tumor growth was significantly repressed by miR-382-3p.

miR-382-3p inhibits SAE1 expression by targeting its 3'-UTR. To further investigate how miR-382-3p represses LA growth, potent miR-382-3p targets were predicted using TargetScan (http://www.targetscan.org/vert_72/) and the predicted targets were subjected to gene ontology analysis using DAVID (https://david.ncifcrf.gov/). It was observed that 18 genes were involved in protein ubiquitination modification and 6 genes were functionally enriched in protein SUMOylation modification. The level of SAE1 protein was examined and it was indicated that 57% (41 out of 72) of patients had increased SAE1 expression in their tumor samples (Fig. 2A and B), and that SAE1 expression levels were negatively correlated with the miR-382-3p levels in tumors (Fig. 2C). Subsequently, the survival data of patients with LA were analyzed online (http://kmplot.com/analysis/index.php?p=background) and it was revealed that patients with low SAE1 expression had a significantly longer survival time (Fig. 2E), suggesting that SAE1 may function as an oncogene that promotes the progression of LA.

To explore whether SAE1 upregulation is directly induced by miR-382-3p downregulation, an SAE1 reporter vector was first constructed. A mutant vector containing 3 replaced nucleotides was also generated to identify the target site of miR-382-3p. As presented in Fig. 3A, relative luciferase activity was significantly repressed by the miR-382-3p mimics and upregulated by the miR-382-3p inhibitor. When 3 out of 7 nucleotides in the miR-382-3p targeting region were mutated, luciferase activity was not repressed by miR-382-3p. These results indicated that miR-382-3p repressed Firefly luciferase expression by targeting the 3'-UTR region of SAE1. To further identify whether endogenous SAE1 is regulated by miR-382-3p, endogenous SAE1 expression was examined in A549 and H1299 cells after transfection with miR-382-3p mimics or inhibitor. It was observed that SAE1 expression was repressed by miR-382-3p and upregulated by an miR-382-3p inhibitor, further indicating that SAE1 is a direct target of miR-382-3p (Fig. 3B). SAE1 protein levels were then examined in xenograft tumors generated from miR-382-3p-overexpressing A549 and H1299. To understand the tumor cell proliferation *in vivo*, the Ki-67 signal was examined by immunohistochemistry. As presented in Fig. 3C, miR-382-3p-overexpressing tumors had reduced SAE1 and Ki-67 levels.

Downregulation of miR-382-3p promotes AKT SUMOylation and phosphorylation. To understand the role of SAE1 upregulation in LA, a full-scale SUMOylation analysis was performed in both tumors and adjacent non-tumor control samples. As presented in Fig. 4A, patients with increased SAE1 expression in the tumor (cases no. 4 and 5 of the 57% of patients with increased SAE1 expression.) exhibited upregulated SUMOylation modification and increased pAKT levels compared to normal tissues.

To identify whether an increase in pAKT resulted from downregulation of miR-382-3p, miR-382-3p was knocked down in A549 and H1299 cells. Proteins modified by SUMO1 were enriched by immunoprecipitation using anti-SUMO1 antibody, and the AKT protein level was examined by immunoblotting. As indicated in Fig. 4B, endogenous miR-382-3p was reduced to 37.1 and 40.7% in A549 and H1299 cells, respectively. SUMOylated AKT levels were increased and pAKT was upregulated. To confirm the activation of the

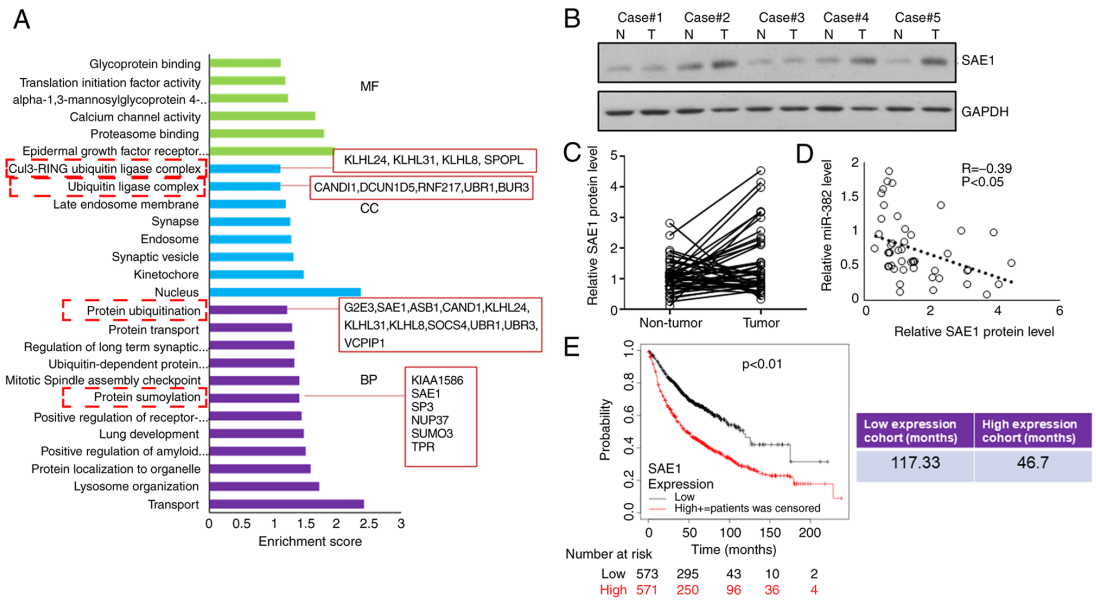

Figure 2. Expression of SAE1, a target of miR-382-3p, is negatively correlated with miR-382-3p levels in tumors. (A) Gene Ontology analysis of predicted miR-382-3p targets. (B and C) SAE1 protein levels in tumor and adjacent non-tumor control samples were examined by immunoblotting. (B) Representative western blots and (C) comparison of SAE1 protein levels between tumor and adjacent non-tumor control samples for each case. (D) Correlation analysis of the SAE1 protein levels and miR-382-3p levels in lung adenocarcinoma tumor samples. (E) Kaplan-Meier curves depicting the overall survival of 1,044 patients with lung cancer. Data were from Kaplan-Meier Plotter. SAE1, small ubiquitin-like modifier 1 activating enzyme subunit 1; miR, microRNA; MF, molecular function; CC, cellular component; BP, biological process; T, tumor tissue; N, normal tissue.

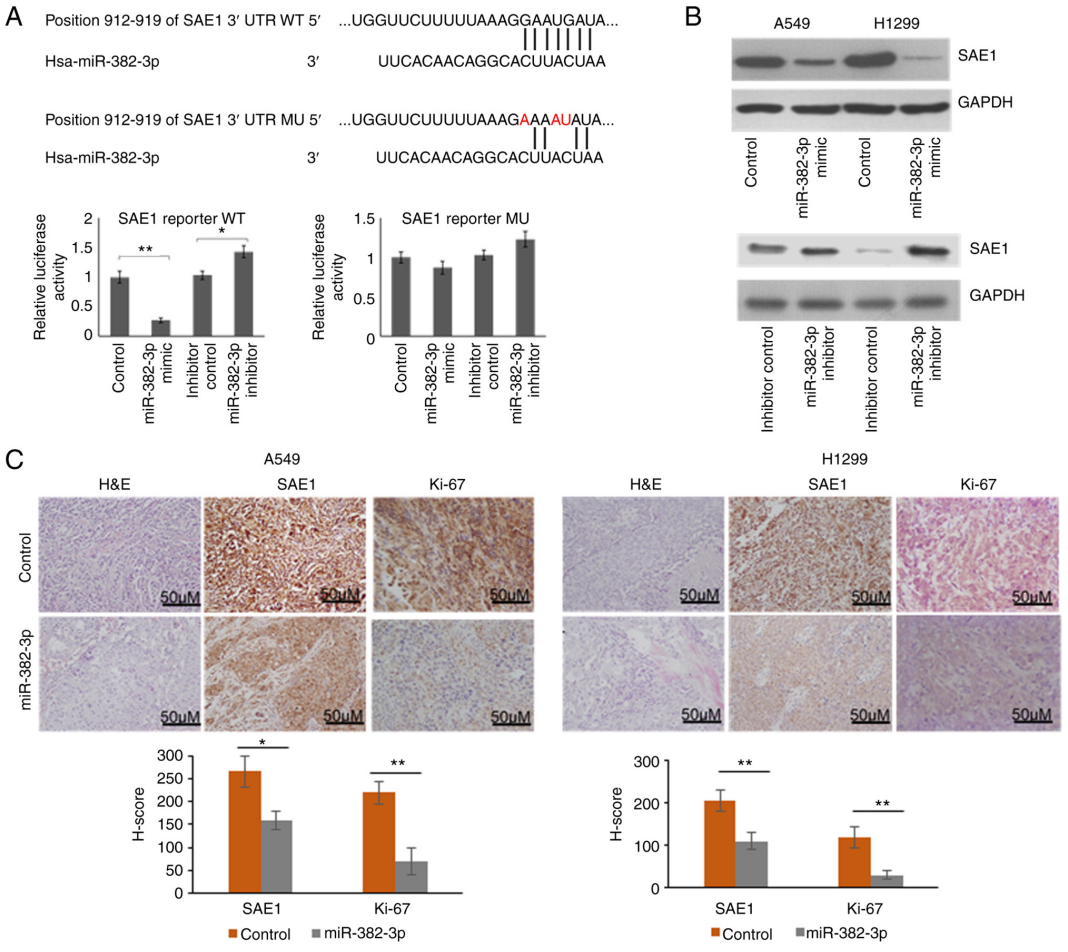

Figure 3. miR-382-3p represses SAE1 expression directly by targeting its 3'UTR. (A) Dual-luciferase assay. (B) miR-382-3p mimics or inhibitor were transfected into A549 and H1299 cells. At 48 h after transfection, the cells were subjected to protein exaction and immunoblotting. (C) The levels of SAE1 and Ki-67 in xenograft tumors generated from miR-382-3p-overexpressing A549 and H1299 cells were examined by immunohistochemistry (scale bars, 50 μM). *P<0.05, **P<0.01. SAE1, small ubiquitin-like modifier 1 activating enzyme subunit 1; miR, microRNA; WT, wild-type; Mut, mutant.

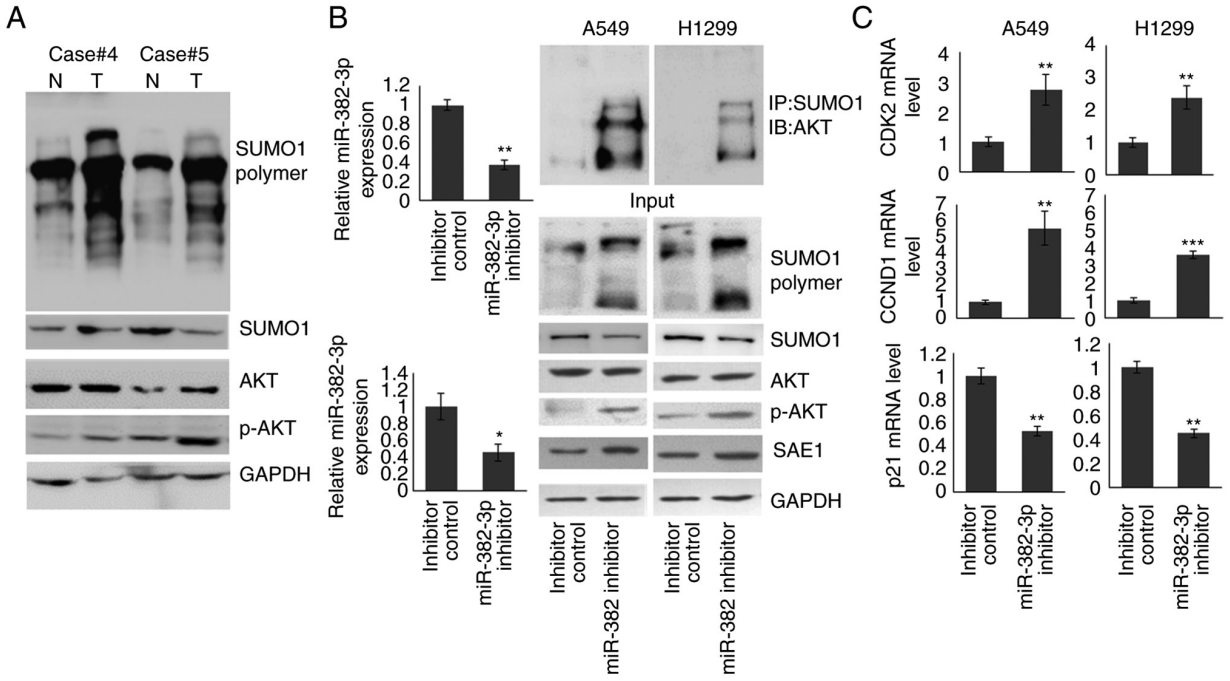

Figure 4. miR-382-3p inhibition upregulates AKT SUMOylation and activates the AKT signaling pathway. (A) Immunoblotting was used to detect the levels of full-scale SUMOylation, SUMO1, AKT and p-AKT in tumor and non-tumor control samples. (B) A549 and H1299 cells were transfected with miR-382-3p inhibitor for 48 h. The cells were then subjected to RT-qPCR and immunoblotting. (C) The expression of AKT signaling downstream genes was examined by RT-qPCR. *P<0.05, **P<0.01, ***P<0.001 vs. control. miR, microRNA; RT-qPCR, reverse transcription-quantitative PCR; p-AKT, phosphorylated AKT; T, tumor tissue; N, normal tissue; IP, immunoprecipitation; IB, immunoblot; CCND1, cyclin D1; CDK2, cyclin-dependent kinase 2; SUMO1, small ubiquitin-like modifier 1.

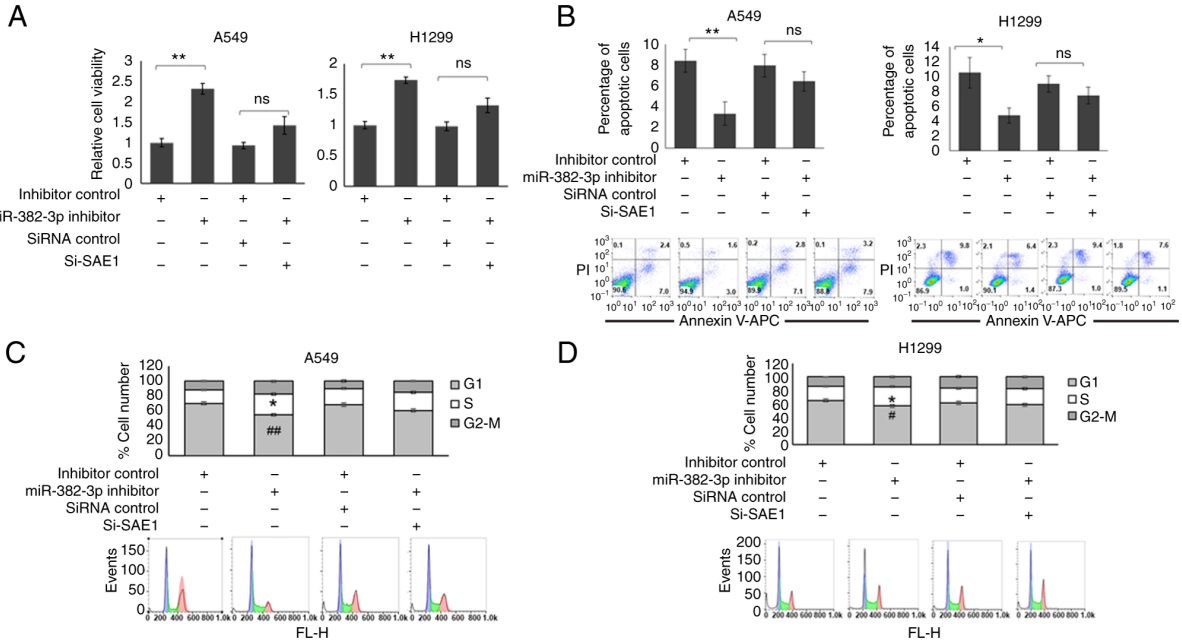

Figure 5. miR-382-3p inhibition promotes proliferation and inhibits apoptosis in lung adenocarcinoma cell lines. A549 and H1299 cells were transfected with miR-382-3p inhibitor, with or without SAE1-specific siRNA for 48 h. (A) The cells were subjected to MTT assays to examine proliferation and viability. (B) Flow cytometric analysis was used to detect cell viability and apoptosis. *P<0.05, **P<0.01. (C and D) Cell cycle analysis of (C) A549 and (D) H1299 cells. *P<0.05 S phase vs. inhibitor control; $^{\#}$P<0.05, $^{\#\#}$P<0.01 G2-M phase vs. inhibitor control. ns, no significance; miR, microRNA; PI, propidium iodide; APC, allophycocyanin; siRNA, small interfering RNA; si-SAE1, siRNA targeting SAE1; SAE1, small ubiquitin-like modifier 1 activating enzyme subunit 1; FL-H, fluorescence-height.

AKT signaling pathway by the miR-382-3p inhibitor, the mRNA levels of three downstream genes were examined. As presented in Fig. 4C, CCND1 and CDK2 expression were significantly increased in miR-382-3p inhibitor-transfected A549 and H1299 cells, while p21 levels were reduced. These results indicated that miR-382-3p inhibition activated the AKT

signaling pathway by promoting AKT SUMOylation and phosphorylation.

Inhibition of miR-382-3p promotes proliferation and inhibits apoptosis in LA cells by upregulating SAE1. To further understand the biological function of miR-382-3p and SAE1 in lung cancer carcinogenesis, A549 and H1299 cells were transfected with a miR-382-3p inhibitor with or without siRNAs specifically targeting SAE1. SAE1 knockdown was confirmed using immunoblotting (Fig. S1). As presented in Fig. 5A, cell viability was increased in the miR-382-3p knockdown A549 and H1299 cells. Although the cell viability was still slightly higher in miR-382-3p and SAE1 double knockdown cells, the difference was not significant. A parallel effect was observed on cell apoptosis. As presented in Fig. 5B, the number of apoptotic cells was reduced in miR-382-3p knockdown cells, while SAE1 and miR-382-3p double-knockdown cells had a similar proportion of apoptotic cells as the control cells. Furthermore, miR-382-3p knockdown A549 and H1299 cells had an increased S-phase population (Fig. 5C and D). SAE1 knockdown partially restored miR-382-3p inhibitor function (Fig. 5C and D).

Discussion

miR-382-3p expression has been known to be downregulated in the peripheral blood of patients with LA, but its direct targets and biological functions have remained elusive (7). In the present study, it was confirmed that miR-382-3p was also downregulated in tumor samples from patients with LA. The direct targets of miR-382-3p were predicted using bioinformatics tools and their interaction was confirmed using a dual-luciferase assay and immunoblotting. It was identified that SAE1, a key component of the SUMO activation complex, is a direct target of miR-382-3p. Knockdown of miR-382-3p in LA cells upregulated SAE1 protein levels and promoted the SUMOylation of AKT, which further promoted cell proliferation and inhibited apoptosis by upregulating AKT downstream genes.

miR-382-5p is the predominant product of the gene encoding miR-382, which acts as a tumor suppressor and is involved in the pathogenesis of various human cancers, including hepatocellular carcinoma, ovarian cancer and osteosarcoma (18-20). However, the role of miR-382-3p in the lung has remained to be fully elucidated. In the present study, it was identified for the first time, to the best of our knowledge, that the downregulation of miR-382-3p in patients with LA contributes to the carcinogenesis of LA via activation of the AKT signaling pathway. miR-382-3p overexpression repressed tumor growth in xenograft mouse models, providing a candidate for LA treatment.

miRNAs are a group of non-coding RNAs that are initially transcribed by RNA polymerase II to form primary transcripts (pri-miRNAs) (21). Pri-miRNAs are then processed through a two-step cleavage mechanism involving two RNase III-class enzymes, Drosha and Dicer, and become mature 21-23 nt-long miRNAs (22). miRNA duplexes are loaded onto Argonaute family proteins and are subsequently unwound to form mature effector complexes that regulate the expression of target mRNAs. One miRNA typically regulates the expression of multiple targets simultaneously. In the present study, only SAE1 was identified as one of the targets of miR-382-3p. Although the importance of SAE1 in the regulatory effect of miR-382-3p on cell proliferation, apoptosis and cell cycle has been confirmed through knockdown experiments, the full roles of miR-382-3p downregulation in the carcinogenesis and processes associated with LA still require to be fully elucidated.

Cells control miRNA levels in multiple ways, including transcription, maturation and degradation. miR-382-3p was identified to be related to the carcinogenesis of LA in the present study, but how miR-382-3p exerts its regulatory roles in lung cancer cells remains to be further investigated.

In conclusion, the present study determined that downregulation of miR-382-3p contributes to the carcinogenesis of LA by upregulating SAE1 and promoting AKT SUMOylation.

Acknowledgements

Not applicable.

Funding

This research was supported by Beijing Gold-Bridge Project (grant no. ZZ19058) and Beijing Xicheng District Excellent Talent Training Funding Project (grant no. 202038).

Availability of data and materials

The datasets used and/or analyzed during the current study are available from the corresponding author on reasonable request.

Authors' contributions

HF was responsible for the conception and design of the study. HF, ZW and WW were involved in data acquisition. HF, ZW and WW were involved in the development of the study methodology, analysis and interpretation of the data. HF was involved in the writing, reviewing and revision of the article and analyzed the relevant literature. All the authors have read and approved the final manuscript. HF, ZW and WW confirmed the authenticity of the raw data.

Ethics approval and consent to participate

The present study was approved by the Human Basic and Clinical Research Ethics Committee of Fuxing Hospital (Beijing, China; approval no. 2018FXHEC-KY-19). All participants provided written informed consent according to the principles of the Declaration of Helsinki prior to sampling. All experiments involving animals were pre-approved by the IACUC of Fuxing Hospital (Beijing, China).

Patient consent for publication

Not applicable.

Competing interests

The authors declare that they have no competing interests.

References

1. Siegel RL, Miller KD and Jemal A: Cancer statistics, 2015. CA Cancer J Clin 65: 5-29, 2015.
2. Chen Z, Fillmore CM, Hammerman PS, Kim CF and Wong KK: Non-small-cell lung cancers: A heterogeneous set of diseases. Nat Rev Cancer 14: 535-546, 2014.
3. Li Q, Liu M, Ma F, Luo Y, Cai R, Wang L, Xu N and Xu B: Circulating miR-19a and miR-205 in serum may predict the sensitivity of luminal A subtype of breast cancer patients to neoadjuvant chemotherapy with epirubicin plus paclitaxel. PLoS One 9: e104870, 2014.
4. Maes OC, Chertkow HM, Wang E and Schipper HM: MicroRNA: Implications for Alzheimer disease and other human CNS disorders. Curr Genomics 10: 154-168, 2009.
5. Xu J, Li Y, Wang F, Wang X, Cheng B, Ye F, Xie X, Zhou C and Lu W: Suppressed miR-424 expression via upregulation of target gene Chk1 contributes to the progression of cervical cancer. Oncogene 32: 976-987, 2013.
6. Farazi TA, Hoell JI, Morozov P and Tuschl T: MicroRNAs in human cancer. Adv Exp Med Biol 774: 1-20, 2013.
7. Fang H, Liu Y, He Y, Jiang Y, Wei Y, Liu H, Gong Y and An G: Extracellular vesicle-delivered miR-505-5p, as a diagnostic biomarker of early lung adenocarcinoma, inhibits cell apoptosis by targeting TP53AIP1. Int J Oncol 54: 1821-1832, 2019.
8. Vivanco I and Sawyers CL: The phosphatidylinositol 3-Kinase AKT pathway in human cancer. Nat Rev Cancer 2: 489-501, 2002.
9. Tsurutani J, Fukuoka J, Tsurutani H, Shih JH, Hewitt SM, Travis WD, Jen J and Dennis PA: Evaluation of two phosphorylation sites improves the prognostic significance of Akt activation in non-small-cell lung cancer tumors. J Clin Oncol 24: 306-314, 2006.
10. Yoshizawa A, Fukuoka J, Shimizu S, Shilo K, Franks TJ, Hewitt SM, Fujii T, Cordon-Cardo C, Jen J and Travis WD: Overexpression of phospho-eIF4E is associated with survival through AKT pathway in non-small cell lung cancer. Clin Cancer Res 16: 240-248, 2010.
11. Li R, Wei J, Jiang C, Liu D, Deng L, Zhang K and Wang P: Akt SUMOylation regulates cell proliferation and tumorigenesis. Cancer Res 73: 5742-5753, 2013.
12. Kessler BM, Bursomanno S, McGouran JF, Hickson ID and Liu Y: Biochemical and mass spectrometry-based approaches to profile SUMOylation in human cells. Methods Mol Biol 1491: 131-144, 2017.
13. Seeler JS and Dejean A: SUMO and the robustness of cancer. Nat Rev Cancer 17: 184-197, 2017.
14. Inamura K, Shimoji T, Ninomiya H, Hiramatsu M, Okui M, Satoh Y, Okumura S, Nakagawa K, Noda T, Fukayama M and Ishikawa Y: A metastatic signature in entire lung adenocarcinomas irrespective of morphological heterogeneity. Hum Pathol 38: 702-709, 2007.
15. Orlans FB: Regulation of animal experimentation: United States of America. Acta Physiol Scand Suppl 554: 138-152, 1986.
16. Guide for the Care and Use of Laboratory Animals. Washington, DC, 1996.
17. Livak KJ and Schmittgen TD: Analysis of relative gene expression data using real-time quantitative PCR and the 2(-Delta Delta C(T)) method. Methods 25: 402-408, 2001.
18. Zhang S, Ge W, Zou G, Yu L, Zhu Y, Li Q, Zhang Y, Wang Z and Xu T: MiR-382 targets GOLM1 to inhibit metastasis of hepatocellular carcinoma and its down-regulation predicts a poor survival. Am J Cancer Res 8: 120-131, 2018.
19. Tan H, He Q, Gong G, Wang Y, Li J, Wang J, Zhu D and Wu X: miR-382 inhibits migration and invasion by targeting ROR1 through regulating EMT in ovarian cancer. Int J Oncol 48: 181-190, 2016.
20. Xu M, Jin H, Xu CX, Sun B, Song ZG, Bi WZ and Wang Y: miR-382 inhibits osteosarcoma metastasis and relapse by targeting Y box-binding protein 1. Mol Ther 23: 89-98, 2015.
21. Kim VN, Han J and Siomi MC: Biogenesis of small RNAs in animals. Nat Rev Mol Cell Biol 10: 126-139, 2009.
22. Okamura K: Diversity of animal small RNA pathways and their biological utility. Wiley Interdiscip Rev RNA 3: 351-368, 2012.